Aalborg Universitet

AALBORG UNIVERSITY

CLIMA 2016 - proceedings of the 12th REHVA World Congress

volume 9

Heiselberg, Per Kvols

Publication date:
2016

Document Version
Publisher's PDF, also known as Version of record

Link to publication from Aalborg University

A Study of Heat Transfer and Pressure Drop on Finned-Tube Heat Exchangers

Waleed A. Abdelmaksoud[#1]and Mahmoud A. Kassem[*2]

[#]*Assistant Professor, Mechanical Engineering Department, Cairo University, Giza, Egypt*
[*]*Associate Professor, Mechanical Engineering Department, Cairo University, Giza, Egypt*
[1]wamarouf@staff.cu.edu.eg

Abstract
There is a need in the heat exchanger industry for accurate guidelines in the heat exchanger design phase. These guidelines can be used to predict the thermal/fluid performance of the heat exchanger that will be manufactured. Accurate prediction for the heat exchanger performance will avoid the cost needed for performing tests in terms of facility and man-hour costs on the heat exchanger prototype before the mass production. Therefore, this paper is devoted to study the thermal/fluid properties on typical compact heat exchanger, which can be found in many HVAC industrial applications. We used the CFD tool to study several factors that can affect the heat exchangers performance, such as the fins spacing and flow inlet velocity conditions. For each of these factors, we estimated the heat transfer rate and the pressure drop in the heat exchanger with the aim of providing an optimum heat exchanger configuration and flow inlet conditions that will provide an enhanced heat transfer rate and reduced amount of pressure drop.

Keywords - Heat exchangers; CFD; heat transfer; pressure drop

1. Introduction

The heat exchanger is a device that is used to transfer the thermal energy (enthalpy) between two or more fluids separated by a solid surface. Common examples of heat exchangers in everyday use are air preheaters, automobile radiators, condensers, and evaporators. The performance of any heat exchanger is measured in terms of flow pressure drop and heat transfer rate that the heat exchanger can handle [1].

The heat transfer rate depends on the heat transfer coefficient, temperature difference between the two fluids, and surface area. Because of the low heat transfer coefficient in some heat exchanger types, the surface area increases via extended surfaces (fins) so it increases the amount of heat transfer and if the volume of heat exchanger in this case is small then it is called compact heat exchanger. The heat exchanger is considered compact if the surface area density on any one fluid side is above about 400 m^2/m^3 [2]. The compact heat exchanger type allows for an increased heat transfer rate, less volume and less weight compared to other heat exchanger types.

The volume and weight of heat exchangers are significant parameters in the overall application and thus may still be considered as economic variables [3-5]. Compact heat exchangers are clearly the preferred choice for applications which require a high heat transfer rate in a limited volume such as air conditioning (AC) devices but the main disadvantage of compact heat exchangers is the higher pressure drop. Many factors affect the heat exchanger performance (heat transfer and pressure drop) such as the face velocity, tubes arrangement, tube spacing, and fin spacing…etc. Some of these factors will be illustrated in the present paper.

Several researches have been published on heat exchangers performance. These researches reported the effect of some factors on the heat exchangers performance. The study in [6] provided a survey for previous published data and correlations. They found that fin spacing is one of the most important parameters in flat-tube geometry heat exchanger and it ranges from 1.4 to 4 mm. The study in [7] reported that fin spacing has negligible effect on heat transfer coefficient and has significant effect on the pressure drop. The study in [8] developed correlations for the pressure drop of a staggered bank of bare tubes (no fins) in cross flow. These correlations give pressure drop as a function of geometry over a range of Reynolds numbers. Heat exchangers can have wet or dry surfaces. A surface is assumed to be wet when its temperature is lower than the fluid's dew point such as in the air-cooling evaporators. The condensate on the surface can have an effect of the heat exchanger performance. The study in [9] found that the colburn factor decreases under wet condition for low Reynolds numbers (Re<2000), and the colburn factor is nearly the same as dry surfaces for high Reynolds numbers (Re>2000). For simplicity, we will study only dry surface heat exchangers type such as the air-cooled condensers in the AC devices and radiators in automobiles. These types of heat exchangers are typically designed with fins on the outside surface because of the low heat transfer coefficient of the air flow.

The aim of the proposed research is to introduce accurate design guidelines (heat transfer and pressure drop correlations) for any dry surface finned-tube heat exchanger. By using the proposed design guidelines, it is expected to reduce and/or eliminate the cost in carry out performance tests on the heat exchanger in terms of facility and man-hour costs before the mass production.

2. Computational Domain and Setup

This section summarizes the CFD model of the studied heat exchanger configuration. Fig. 1 shows a schematic view for the heat exchanger, which has flat fins placed on 4-row tubes in an inline arrangement. The 4-row tubes heat exchanger was selected because many researches in the literature were

performed on that type of heat exchanger (e.g. [10-11]). The heat transfer from the tubes and fins is rejected to the inlet cold air which becomes hotter at the exit. Heat exchangers may have hundreds of fins on the tubes and the spacing between fins varies differently from heat exchanger to another. This fin spacing can affect the heat exchanger performance. Therefore, the fin spacing is a major variable parameter in the current study. Also, the air velocity affects the heat transfer coefficient and the pressure drop on the heat exchanger. So, the air flow velocity is also another variable parameter in the current study.

The heat exchanger may contain several tubes in the vertical direction and the air flow characteristics are nearly identical between each pair of vertical tubes passage. Therefore, it was suggested to model only one passage of air flow so the required number of grid cells is significantly reduced and this approach allowed to use fine grids in the small suggested computational domain. Fig. 2 shows an isometric view for the studied computational domain, which was built using the grid generation software Gambit 2.4.6. The domain size: $X = 190.50$ mm, $Y = 31.75$ mm and $Z = 3.73$ mm (or 2.68 or 2.04 mm). The Z-dimension (fin spacing variable parameter) varies according to the case number (discussed later). The 3.73, 2.68 and 2.04 mm represents cases for 6, 8 and 10 fins/inch. The total number of grid cells is 827925 when $Z = 3.73$ mm and is 697200 when $Z = 2.68$ mm and is 610050 when $Z = 2.04$ mm. The tubes diameter (D) is 15.88 mm and the spacing between tube-centers in the X-direction is 47.63 mm (or 3D).
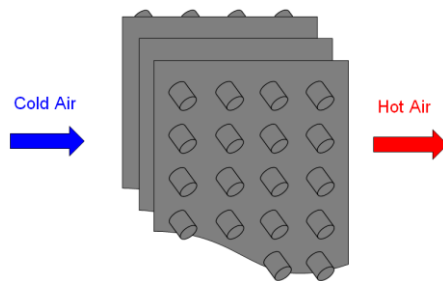

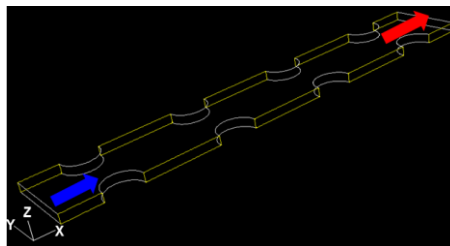Fig. 1 A cutaway view of a 4-row tubes heat exchanger

Fig. 2 Isometric view of the computational domain

All the CFD simulations were performed using a commercial CFD software package (ANSYS FLUENT version 14). The flow was assumed incompressible, and the Reynolds-Averaged Navier-Stokes (RANS) equations were solved with the SIMPLE algorithm. All convective transport terms were discretized using a 2nd order-accurate upwind scheme, while the diffusion terms were discretized using a 2nd order-accurate central-difference scheme. Pressure interpolation was achieved with a 2nd order-accurate scheme. The widely-accepted two-equation standard k-ε turbulence model coupled with enhanced wall treatment was employed. Table 1 summarizes the inputs used in the CFD simulations. Buoyancy was modeled using the incompressible ideal gas method. The incompressible ideal gas model treats the air density as a function of the local temperature and the operating pressure field (not on the local relative pressure) using the ideal gas law for an incompressible flow.

Table 1. CFD input boundary conditions used in the study

Parameter	Value
Cases	Steady and 3-D calculations
Turbulence model	Standard k-ε model coupled with enhanced wall treatment
Buoyancy	Incompressible ideal gas model
Walls	Cylinders: constant temperature = 55°C
	Fin surfaces: constant temperature = 55°C
Air inlet conditions	Velocity: conditions according to the case listed in Tables 2
	Temperature: 30°C
	Turbulence: I = 6%, L = 0.3 mm
Air exit conditions	Outflow boundary condition

Twelve CFD cases are presented in this paper. Two major variable parameters are presented in these 12 cases. As shown in Table 2, the first parameter is the fin spacing that goes from 3.73 mm to 2.04 mm (or from 6 fins per inch to 10 fins per inch) while the second parameter is the inlet velocity or face velocity that goes from 4 m/s to 10 m/s. Note, all the 12 cases use the input data listed in Table 1. The results from these CFD cases will be used to investigate the effect of the fin spacing and the inlet velocity on the heat exchangers performance. The results will be demonstrated in a few useful correlations that will be applicable to typical heat exchangers.

Table 2. CFD case studies for studying the performance of the heat exchanger

Case	Fin Spacing, mm	Inlet Velocity, m/s
1		4
2	3.73 (6 fins/inch)	6
3		8
4		10
5		4
6	2.68 (8 fins/inch)	6
7		8
8		10
9		4
10	2.04 (10 fins/inch)	6
11		8
12		10

• All the cases have the same CFD inputs listed in Table 1.

3. Mesh Generation and Near-Wall Treatment

Gambit 2.4.6 was used to generate the 3-D mesh of the CFD domain shown in Fig. 2. The simplest method is to build a mesh that has uniform grid in the entire CFD domain. But, care must be taken for the grid distribution near the wall region because of the turbulent flows generated near the walls. The mesh distribution near the wall region depends on the near-wall treatment approach used in the CFD model (wall functions or near-wall modeling). Selecting one of those two approaches depends on the dimensionless number y^+. Values of $y^+ \sim 30$ up to $y^+ \sim 500 - 1000$ are most desirable for wall functions, while values of $y^+ \sim 1$ (or $y^+ < 5$) are most desirable for near-wall modeling (e.g. [12-14]). Near-wall grid size corresponding to y^+ in the range of 5 to 30 should be avoided when using the turbulence models available in FLUENT. The wall y^+ is calculated in CFD to describe how coarse or fine the near-wall mesh is. It is expressed as,

$$y^+ = \frac{u^* y}{\nu} \tag{1}$$

where y is the distance from the wall to the center of the adjacent cell, ν is the fluid kinematic viscosity and u^* is the friction velocity or shear velocity and is defined as,

$$u^* = \sqrt{\tau_o / \rho} \tag{2}$$

In the above expression, τ_o is the wall shear stress and ρ is fluid density. As mentioned before, the region near the wall can be solved in two different approaches; wall functions or near-wall modeling. The wall functions approach uses semi-empirical formulas called wall functions and is used in the different k - ε models [14]. These functions are used to link the solution between the wall and the fully turbulent flow region instead of resolving the viscosity affected region (buffer layer and viscous sublayer), which reduces the computational cost. This approach is popular in high Reynolds number flows or coarse grid near the wall region. On the other hand, in the detailed near-wall (or enhanced wall treatment) modeling approach, the mesh near the wall must be fine enough in order to resolve the viscosity affected region. The near-wall modeling is a good approach for low Reynolds number flows but requires very fine mesh.
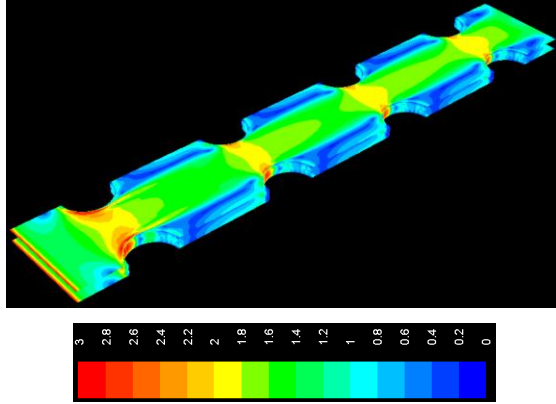

Fig. 3 Wall y+ on the cylinders and fin surfaces

In the present paper, the near-wall (or enhanced wall treatment) approach was employed in the CFD analysis. To achieve the $y^+ \sim 1$ condition, we used very fine grid near the walls (cylinders and fin surfaces). The grid cells size near the walls are 0.08 mm and the cells grow smoothly with a stretching ratio of $\sim$ 1.2 to reach grid cells size of $\sim$ 0.35 mm far from the walls. The CFD simulations were performed with the boundary conditions described the previous section. Fig. 3 shows the contours of y^+ produced from Case 12 that is described in Table 2, which has the high inlet velocity (10 m/s). This high inlet velocity results in high y^+ because the high Reynolds number. The y^+ generated from Case 12 is expected to be similar to the y^+ generated from Case 4 and Case 8. As shown in Fig. 3, the contours indicate acceptable y^+ values ($y^+ < 3$) on the cylinders and fin surfaces (top and bottom fins). Therefore, the enhanced wall treatment approach can be successfully employed in all the CFD simulations.

4.   Results and Discussions

The results from the 12 CFD cases described in Tables 1 and 2 are presented in this section. Fig. 4 shows the temperature and static pressure contours in a horizontal plane at height of Z/2 (half the fin spacing). In all the CFD cases, the cold and high pressure air flow enters the passage to receive heat from the cylinders and fin surfaces then exits in warm and low pressure conditions. The air enters with uniform temperature of 30°C and high pressure (varies from case to case). The inlet pressure changes because the different flow resistance in each case and the fixed zero pressure condition at the center of the exit area.

Two observations can be noticed from the temperature distribution results in Fig. 4. First observation, the increase in the inlet velocity (face velocity) results in slight decrease in the exit temperature. For example, the inlet velocity that increases from 4 to 10 m/s in Cases 1 to 4 (cases of 6 fins/inch) resulted in a decrease of ~ 2.5°C at the exit. Nearly the same results are obtained in Cases 5 to 8 (cases of 8 fins/inch) and Cases 9 to 12 (cases of 10 fins/inch). The decrease in the temperature is a result of increase in the heat transfer coefficient due to the increase in the air velocity. Second observation, the decrease in the fin spacing increases the air temperature level between the fin surfaces so the exit air temperature becomes warmer. This observation can be clearly noticed in the short temperature potential core produced in the cases of 10 fins/inch. In these cases, the temperature potential cores length don't pass the first row of tubes while in the cases of 8 and 6 fins/inch, the temperature potential cores length do pass it. The reason for this increase in the temperature level is the increase of heat transfer rate due to the increase of total surface area (or number of fins).

On the other hand, two observations can be noticed from the pressure distribution results in Fig. 4. First observation, the increase in the inlet velocity results in a significant increase in the pressure drop. For example, the inlet velocity that increases from 4 to 10 m/s in Cases 1 to 4 (cases of 6 fins/inch) resulted in an increase of pressure drop ~ 86 Pa to 407 Pa. This result nearly agrees with Darcy-Weisbach equation, which states that the pressure drop is proportional to the square of the air velocity in a pipe. Nearly the same results are obtained in the cases of 8 and 10 fins/inch. The increase in pressure drop increases the fan power consumption that increases the total cost of the system. But, as explained in the previous paragraph, the increase of air velocity increases the heat transfer coefficient so the surface area can be decreased so the total cost can be reduced. Describing this in another way, the increase of air velocity decreases the surface area cost and increases the fan power cost. So, there must be an optimum air velocity that gives a minimum total cost.

The second observation from pressure contours in Fig. 4 is that the decrease in fin spacing increases the pressure drop. For example, the pressure drop in Case 8 is higher than in   Case 4 by ~ 100 Pa. This increase

in the pressure is mainly due reduction of the inlet hydraulic diameter (Darcy-Weisbach equation).

After this short discussion for the effect of the inlet air velocity and fin spacing on the heat exchangers performance (heat transfer and pressure distributions), we performed further analysis to display the results from the 12 CFD cases in dimensionless results so the outputs can be useful for any typical heat exchanger. Fig. 5 shows the dimensionless Nusselt number versus Reynolds number at the three fin spacing values. The calculated Nusselt number and Reynolds number in these displayed results are based on the tubes diameter (D = 15.88 mm). The Nusselt number (Nu), defined as Nu = h D / k, where h is the heat transfer coefficient and k is the thermal conductivity of the air. The Reynolds number (Re), defined as Re = V D/ ν, where V is the inlet velocity and ν is the fluid kinematic viscosity.

The results from Fig. 5 illustrate that: (1) the Nusselt number increases linearly as the Reynolds number (or inlet velocity) increases at a given fin spacing, and (2) the Nusselt number is essentially independent of fin spacing (2.04-3.73 mm or 10-6 fins/inch) at a given inlet velocity. Using to the CFD results shown in Fig. 5, we developed a useful correlation that can be used for estimating the heat transfer rate in typical heat exchangers. The following correlation relates the Nusselt number to the Reynolds number,

$$Nu = 18 + 0.006 \, Re \tag{3}$$

We found a maximum error of 1.5% between the calculated Nu number using Equation 3 and the estimated Nu number from the CFD results.

Regarding the pressure drop, Fig. 6 shows the dimensionless pressure coefficient versus Reynolds number at the three fin spacing values. The pressure coefficient (Cp), defined as Cp = ΔP / 0.5 ρV^2, where ΔP is the pressure difference between the inlet and exit conditions. The results from Fig. 6 illustrate that: (1) the pressure coefficient decreases non-linearly as the Reynolds number (or inlet velocity) increases at a given fin spacing, and (2) the pressure coefficient increases as the fin spacing (Z) decreases at a given inlet velocity.

Using to the CFD results shown in Fig. 6, we developed a useful correlation that can be used for estimating the pressure drop in typical heat exchangers. The following correlation relates the dimensionless pressure coefficient (Cp) to the Reynolds number (Re) and the dimensionless fin spacing (Z/D),

$$Cp = 52.65 \, Re^{-0.337} \left(\frac{Z}{D} \right)^{-0.746} \tag{4}$$

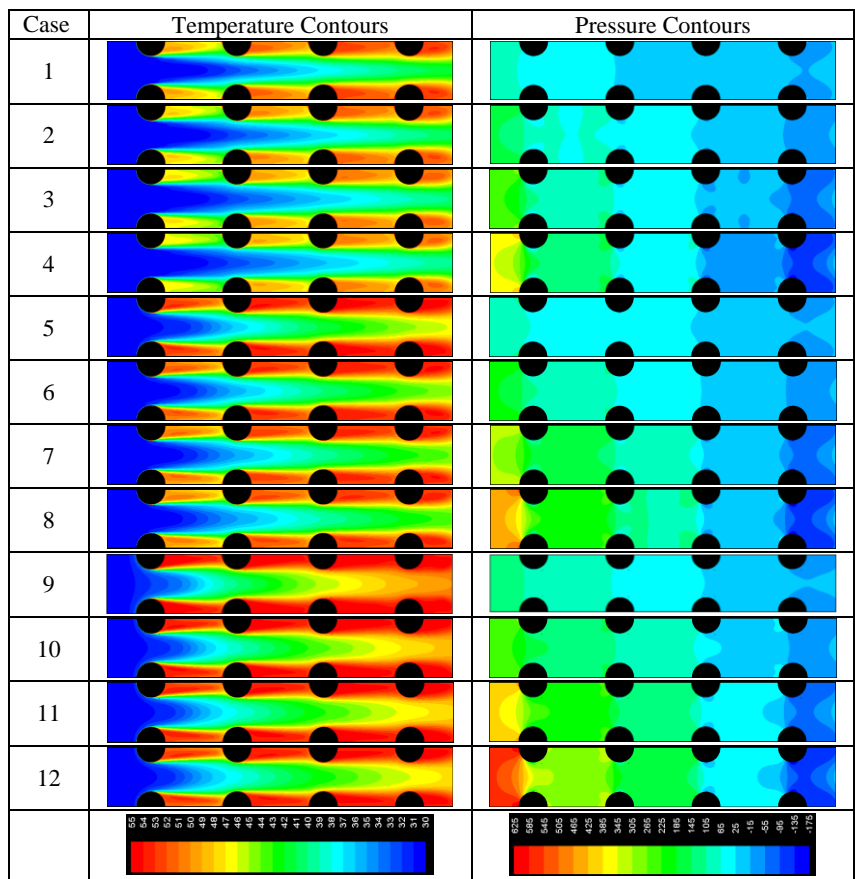We found a maximum error of 4% between the calculated Cp using Equation 4 and the estimated Cp from the CFD results.

Case	Temperature Contours	Pressure Contours
1		
2		
3		
4		
5		
6		
7		
8		
9		
10		
11		
12		

Temperature scale: 55 54 53 52 51 50 49 48 47 46 45 44 43 42 41 40 39 38 37 36 35 34 33 32 31 30

Pressure scale: 625 585 545 505 465 425 385 345 305 265 225 185 145 105 65 25 -15 -55 -95 -135 -175

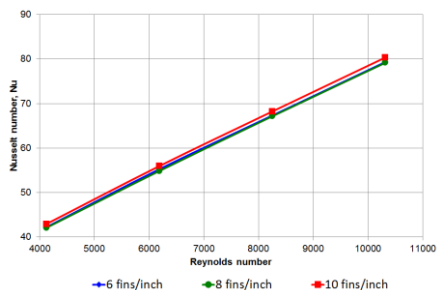Fig. 4 Temperature and pressure contours in a horizontal plane at height of Z/2

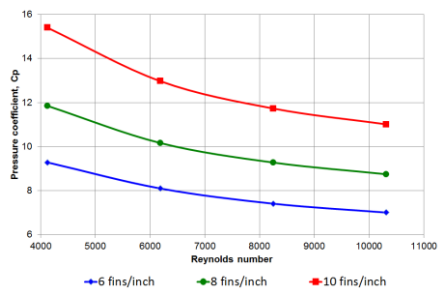Fig. 5 Effect of Reynolds number and fin spacing on the Nusselt number

Fig. 6 Effect of Reynolds number and fin spacing on the pressure coefficient

5. Comparison with Staggered Arrangement

In this section we briefly compare the results obtained in the previous section (for inline tube arrangement) against results obtained for staggered tube arrangement. For the staggered arrangement, we used the same boundary conditions and computational domain size for the 12 CFD cases presented before except that we just changed the location of the tubes to form a staggered arrangement as shown in the following figure.
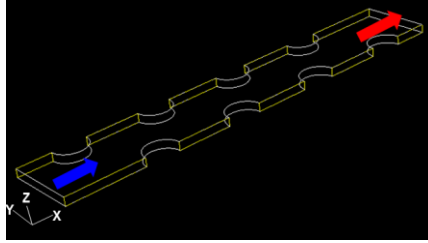

Fig. 7 Isometric view for the staggered tube arrangement

Similar to the results presented in Fig. 5 and 6, we present the results of the new staggered arrangement in Fig. 8 and 9. We observed that insignificant change in the Nusselt number compared to the inline arrangement. But, significant reduction (nearly 10%) in the pressure coefficient is observed. The reason is mainly due to the high maximum velocity found in the inline arrangement. Thus, for staggered arrangement, we suggest to use the same correlations presented in Equations 3 and 4 but with the correction of the ~ 10% for the pressure coefficient only. We expect that this conclusion will be different if we changed the surface-to-volume ratio of the heat exchanger. The effect of surface-to-volume ratio will be discussed in future research.
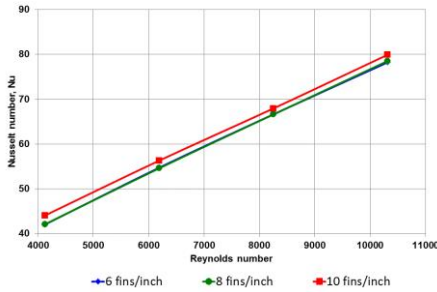

Fig. 8 Effect of Reynolds number and fin spacing on the Nusselt number for staggered arrangement
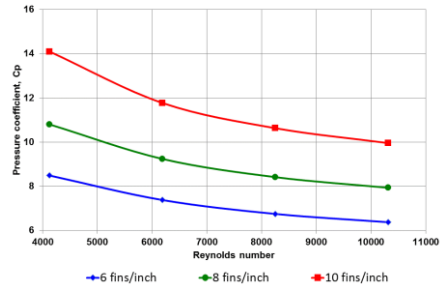

Fig. 9 Effect of Reynolds number and fin spacing on the pressure coefficient staggered arrangement

6. Summary and Conclusions

Twelve CFD cases were studied to investigate the effect of the inlet velocity (face velocity) and the fin spacing on the characteristics (heat transfer and pressure drop) of typical compact finned-tube heat exchanger. The study was performed on both inline and staggered tube arrangements. The results from the 12 cases were presented in the dimensionless Nusselt number and the pressure coefficient. Using these results, two useful correlations were developed for estimating the heat transfer and the pressure drop for typical finned-tube heat exchangers. These two correlations illustrate that the Nusselt number is essentially independent of the fin spacing while the pressure coefficient increases as the fin spacing decreases. Also, as the inlet velocity increases, the Nusselt number linearly increases while the pressure coefficient non-linearly decreases.

References

[1] Tomasz Sobota. Experimental Prediction of Heat Transfer Correlations in Heat Exchangers. Cracow University of Technology Poland. (2011) pp. 293–307.

[2] R. K. Shah and D. P. Sekulic. Handbook of Heat Transfer Applications: Chapter 17. 3rd edition. McGraw-Hill. New York. USA. (1998).

[3] J. P. Holman. Heat Transfer. 10th edition. McGraw-Hill. New York. USA. (2009).

[4] H. Shokouhmand, M. R. Salimpour and M. A. Akhavan-Behabadi. Experimental Investigation of Shell and Coiled Tube Heat Exchangers Using Wilson Plots. International Communications in Heat and Mass Transfer. Vol. 35 (2008) pp. 84–92.

[5] T. J. Rennie and V. G. S. Raghavan. Effect of Fluid Thermal Properties on the Heat Transfer Characteristics in a Double-Pipe Helical Heat Exchanger. International Journal of Thermal Sciences. Vol. 45 (2006) pp. 1158–1165.

[6] Y. G. Park and A. M. Jacobi. Air-Side Performance Characteristics of Round and Flat-Tube Heat Exchangers: A Literature Review, Analysis and Comparison. Air Conditioning and Refrigeration Center. University of Illinois. (2001).

[7] C. C. Wang, Y. J. Chang, Y. C. Hsieh and Y. T. Lin. Sensible Heat and Friction Characteristics of Plate Fin-and-Tube Heat Exchangers Having Plane Fins. International Journal of Refrigeration. Vol. 4 (1996) pp. 223-230.

[8] A. Zukauskas and R. Ulinskas. Banks of plain and finned tubes: Heat Exchanger Design Handbook. Begell House Inc. New York. (1998) pp. 2.2.4-1– 2.2.4-17.

[9] C. C. Wang, Y. C. Hsieh and Y. T. Lin. Performance of Plate Finned Tube Heat Exchangers Under Dehumidifying Conditions. Journal of Heat Transfer. Vol. 119 (1997) pp. 109-117.

[10] J. Y. Yang and J. T. Lai. Numerical and Experimental Analysis of Heat Transfer and Fluid Flow in 3-D Circular Finned-Tube Heat Exchangers. International Conference in Mineral & Metal Processing and Power Generation. (1997).

[11] F.C. McQuiston. Correlation for Heat, Mass and Momentum Transport Coefficients for Plate-Fin-Tube Heat Transfer with Staggered Tube. ASHRAE Transactions. vol. 84 (1978) pp. 294-308.

[12] A. Gerasimov. Modeling Turbulent Flows with FLUENT. Europe. ANSYS Inc. (2006).

[13] B. Blocken, T. Stathopoulos and J. Carmeliet. CFD Simulation of the Atmospheric Boundary Layer: Wall Function Problems. Journal of Atmospheric Environment 41(2007) pp. 238-252.

[14] ANSYS. ANSYS Fluent User's Guide. Canonsburg: ANSYS. (2011).